

# Soil evolution along an alluvial-loess transect in the Herat Plain, western Afghanistan

Farsila MAHMOUDIAN<sup>1</sup>, Alireza KARIMI<sup>2\*</sup>, Omid BAYAT<sup>2</sup>

<sup>1</sup> Department of Soil Science, Faculty of Agriculture, Herat University, Herat 3001-272806, Afghanistan;

<sup>2</sup> Department of Soil Science, Faculty of Agriculture, Ferdowsi University of Mashhad, Mashhad 9177948974, Iran

**Abstract:** Afghanistan is located in the Eurasian loess belt, however, there is little information on the soils in the area. Loess has covered the Herat Plain in western Herat City, Afghanistan. Despite the diversity of landform and parent material, there is no information on the soil and landform evolution in this area. The objectives of this study were to identify the soils along a transect of different landforms in the Herat Plain and determine the role of geomorphic processes on the soil and landform evolution. Five pedons from an alluvial fan, the depression between alluvial fan and piedmont plain, saline and non-saline piedmont plains, and the flood plain of the Harirod River, were sampled. Then, the physical-chemical properties, mineralogy, and micromorphology of the samples were determined. Results showed that the soil parent material in the piedmont plain is loess, whereas, in the flood plain it is a combination of loess and river alluvial sediments. Calcification, lessivage, salinization, and gleization are the most important pedogenic processes. The calcification and lessivage appear to be the result of a wetter climate during the late Quaternary, whereas the present topography causes the gleization and salinization. Clay coatings on carbonate nodules and iron nodules are abundant pedofeatures in the Btk (argilllic-calcic) horizon. Iron oxides nodules are common in the soils of the flood plain. The formation of palygorskite in both alluvial- and loess-derived soils implies the onset of aridity and the trend of increase in environmental aridity in the region. It seems that after the formation of a well developed paleosol on the alluvial fan in a more humid climate in the past, the piedmont plain has been covered by loess deposits, and the calcification, gleization, and salinization cause the formation of weakly developed surficial soils. This study highlights the role of the late Quaternary climatic changes on the evolution of landforms and soils in western Afghanistan.

**Keywords:** alluvial fan; loess-derived soils; paleosol; gleization; Harirod River

**Citation:** Farsila MAHMOUDIAN, Alireza KARIMI, Omid BAYAT. 2022. Soil evolution along an alluvial-loess transect in the Herat Plain, western Afghanistan. *Journal of Arid Land*, 14(11): 1317–1330. <https://doi.org/10.1007/s40333-022-0034-8>

## 1 Introduction

Afghanistan in western Asia is a landlocked country that is bordered by the Hindu Kush and Himalaya mountains in the east and the deserts of Iran in the west (Ellicott and Gall, 2003; Ahmadi, 2021). Late Cenozoic tectonic movements and the uplift of the Hindu Kush and Himalaya mountains, in combination with the Quaternary climatic changes, resulted in remarkable landscape diversity in the country. The complex patterns of mountain slopes, valleys, and plains created different bioclimatic regions and associated soils in Afghanistan (Salem and Hole, 1969; Ellicott and Gall, 2003; Rahmani, 2014; Ahmadi, 2021).

\*Corresponding author: Alireza KARIMI (E-mail: Karimi-a@um.ac.ir)

Received 2022-06-02; revised 2022-10-14; accepted 2022-10-28

© Xinjiang Institute of Ecology and Geography, Chinese Academy of Sciences, Science Press and Springer-Verlag GmbH Germany, part of Springer Nature 2022

Salem and Hole (1969, 1973) studied factors of soil formation and physical-chemical properties of the main groups of soils in eastern and southern Afghanistan, and they concluded that alluvium, colluvium, and loess deposits are the main parent materials of the soils. The first digital soil map for the six northern provinces of Afghanistan was prepared by Rahmani (2014) using artificial neural networks and geostatistical approaches. Similarly, Wali et al. (2021) studied soils in the Khost Province, southeastern Afghanistan, and developed the first digital map for the soils of the region. They found that the soils of the Khost Province are Entisols, Aridisols, and Inceptisols. The main soil in Afghanistan are Entisols, Aridisols, Inceptisols, Alfisols, and Mollisols, and the most developed soils occur in the eastern part of the country, which are affected by summer monsoon rainfalls (Ahmadi, 2021).

Loess deposits and associated soils in northern Afghanistan were investigated by several authors. The soils, developed in calcareous loess in the Kunduz region of northern Afghanistan are young (Bal and Buursink, 1976). The collapse and failure of loess deposits in the Badakhshan region, northeastern Afghanistan, was investigated by Shroder et al. (2011). They found that these processes were controlled by moisture content, structure, and composition of loess deposits as well as slope of the underlying bedrock.

Based on remote sensing techniques, Evenstar et al. (2018) studied that landscape evolution in southern Afghanistan is chiefly controlled by the Quaternary climatic changes. They also found that the terraces of the Sistan paleolake correlate well with glacial-interglacial cycles over the last 800 ka. Li et al. (2019) studied the relationships between atmospheric patterns, dust activity, and loess deposition in the Afghan-Tajik Basin, and found that the difference of air surface pressure between the Caspian Sea and the Hindu Kush Mountains was a controlling factor for dust deposition in the basin during the Quaternary.

The few geomorphological and pedological studies to date have been mainly researched by remote sensing techniques without field survey, due to conflicts and socio-political issues. Thus, the objectives of this study were to: (1) identify the soils along a topographic transect from alluvial fans to the floodplain of the Harirod River in the Herat Plain; (2) determine the role of geomorphic processes on the soil and landform evolution; and (3) compare the status of soils in the study area with similar regions in the world.

## 2 Methods and materials

### 2.1 Study area

The Herat Plain is located in the western part of the Heart City, Afghanistan (Fig. 1). The Herat Plain in western Afghanistan has extensive agricultural lands, especially around the Harirod River. Herat-Frah region is an extension of the Iranian Plateau, which consists of mountain ranges and low hills, and drained by the Harirod and Khashroud rivers (Dupree, 1980). Although Paleozoic crystalline and metamorphic rocks with Mesozoic sedimentary deposits (e.g., limestone and sandstone) are the dominant lithologies of the region (Dupree, 1980), most of the region's surface is covered by the late Pleistocene loess (Fig. 1b), though alluvium deposits are exposed adjacent to the mountains and river banks of the Harirod River (Bohannon and Lindsay, 2007).

The climate of the area is arid, with mean annual precipitation (MAP) of roughly 210 mm and an average annual temperature of about 16.1°C (Dupree, 1980; Ellicot and Galls, 2003). The rainfall pattern is strongly seasonal, and mainly occurs during the cold season. In general, the climate of Southwest Asia is under the influence of three major climatic systems: the Siberian High, the Subtropical High, and the Mediterranean Depression, and the latter is the source of rainfall in the area during cold seasons (Dupree, 1980; Cullen, 2005). However, the summer Indian monsoon occasionally affects the southern and eastern parts of the country (Dupree, 1980). The soil temperature regime of the study area is thermic, and the soil moisture regime is aridic, though areas along water sources may be aquic due to saturation from surface (episaturation) or ground water (endosaturation).

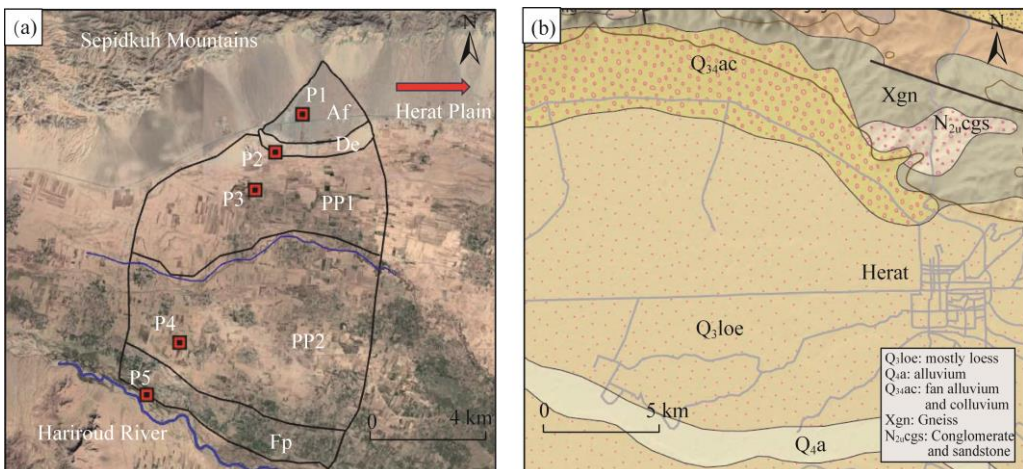


**Fig. 1** (a), location of the study area and the studied soil pedons in the geomorphic surfaces in southern Herat Plain, western Afghanistan; (b), the geology of the study area from Bohannon and Lindsay (2007). P1–P5, soil pedons; Af, alluvial fan; De, depression; PP1, saline piedmont plain; PP2, non-saline piedmont plain; Fp, flood plain.

## 2.2 Landform and sampling

Based on the basin and range geomorphic structure of the area, we selected a transect from the Sepidkuh Mountains to the Hariroud River. The transect contains a piedmont, piedmont plain, and floodplain (Fig. 1a). An alluvial fan (Af) extends across the piedmont of the Sepidkuh Mountains. There is a small depression at the junction of the alluvial fan and piedmont plain, and the runoff from the alluvial fan accumulates in this depression and causes temporary ponding and saturation of the soil. The piedmont plain is composed of two different geomorphic surfaces, including saline (PP1) and non-saline (PP2) units (Figs. 1a and 2). The PP2 located between the seasonal Karabar River and the Hariroud River. It appears that the hydrological gradient caused by a high groundwater table, and consequently aquic conditions. The flood plain of the Hariroud River is the last landform on the studied transect (Fig. 1a).

Five representative pedons (one pedon in each landform) were excavated and described using the criteria of Schoeneberger et al. (2012) and classified (Soil Survey Staff, 2014). Both bulk and undisturbed samples were taken from genetic horizons for laboratory analyses.

## 2.3 Laboratory analyses

### 2.3.1 Physical and chemical analyses

Soil samples were air-dried and passed through a 2-mm sieve. The soil color of dried samples of the <2 mm fraction was determined under natural light using the Munsell color chart. Values of redness rate (RR) were calculated using the dry color, and the equation was proposed by Torrent and Barrón (1993).

$$RR = ((10-H) \times C)/V, \quad (1)$$

where H is the converted Munsell hue (figure preceding YR (yellow-red)); C and V are the chroma and value numbers, respectively. Hematite is a very strong pigment agent in the soils, therefore, RR is usually correlated with the hematite content (Torrent and Barrón, 1993; Bech et al., 1997).

The pH was measured in a saturated paste, and electrical conductivity (EC) was measured in the saturation extract (Rhoades, 1996; Thomas, 1996). The calcium carbonate equivalent (CCE) was determined by acid neutralization (Allison, 1960), and organic carbon (OC) was determined by the Walkley-Black wet digestion method (Nelson and Sommers, 1982). Pedogenic iron (Fe<sub>d</sub>) was extracted by citrate-dithionite using the method of Mehra and Jackson (1960) and measured using atomic spectrometry. Particle size distribution was determined using the hydrometer method

(Gee and Bauder, 1986).

### 2.3.2 Mineralogy and micromorphology analyses

For clay mineralogical analysis, samples were washed with distilled water to remove soluble salts and then treated with sodium acetate-acetic acid buffer (pH value was adjusted to 5.0) in the water bath at 95°C to react and destroy carbonates. The organic matter and manganese oxide were removed by 30% H<sub>2</sub>O<sub>2</sub>, and iron oxides were destroyed by dithionite-citrate-bicarbonate method (Mehra and Jackson, 1960). We separated the clay fraction using a centrifuge according to Kittrick and Hope (1963), and the clay particles were saturated by MgCl<sub>2</sub> and KCl solutions. Two slides of oriented clay saturated with Mg and K were prepared. Mg-saturated (Mg-sat) samples were solvated with ethylene glycol (Mg-EG), and K-saturated (K-sat) samples were heated up to 550°C for 2 h (K-550). X-ray diffraction (XRD) patterns obtained using a Siemens D5000 diffractometer with a monochromator and Cu-K $\alpha$  radiation (30 mA and 40 kV). We identified clay minerals according to Moore and Reynolds (1997) and Dixon and Schulze (2002). Thin sections prepared using standard methods, and the micromorphological descriptions followed the terminology of Stoops (2003) and interpretations of Stoops et al. (2018).

## 3 Results

Soil-landform relationships for the transect and the physical-chemical properties of the soils, are given in Figure 2 and Table 1, respectively.

### 3.1 Parent materials of the soils

Based on the particle size distribution (Table 1) and landform positions (Figs. 1a and 2), the soils have developed on three different types of parent materials: coarse alluvium within the alluvial fan (Af surface), loess deposits in the piedmont plain (PP1 and PP2 surfaces), and a combination of loess and fluvial sediments in the flood plain (Fp surface).

Alluvial fan deposits line the front of the Sepidkuh Mountains and towards the Herat Plain (Fig. 1a). Fan deposits are generally coarse-grained and poorly sorted, and are the result of depositional events during unstable phases of landscape (Blair and McPherson, 2009). The pedon 1 in the alluvial fan contains high gravel contents (45%–73%), and the sand fraction is the dominant particle size (40%–77%) in the fine earth fraction (Table 1).

According to the geological map of the region (Fig. 1b), the late Quaternary loess deposits covered the piedmont plain of the region. Silt is the dominant particle in pedons 2 and 3, with concentrations in the <2 mm fraction of up to 72% (Table 1). Sand content in the Az horizon (Fig. 2) of pedon 2 is 59%, and is considerably higher than the underlying horizons. The higher sand in this horizon is apparently due to transportation from the adjoining alluvial fan. Pedon 4 has also formed on the loess deposits, and is characterized by a low sand content. However, the silt in this soil decreases due to an increase in the clay fraction, likely due to change in the depositional setting of this site. In the flood plain, sand content is distinctly higher than in pedons 4 and 5, indicating the mixing of the sediments from the loess and flood plain.

In order to separate alluvial and loess derived soils, we calculated sand/silt+clay ratios for the studied soils. As illustrated in Figure 3, the values of this index in loess-rich pedons (pedons 2, 3, and 4) are about 0.2, except for the A horizon of pedon 2. The higher ratio in the latter horizon is due to surface runoff processes from the upslope of the alluvial fan. The ratio is the highest in pedon 1 that contains more sand than other pedons due to its geomorphic position.

### 3.2 Morphological and physical-chemical properties of the soils

In pedon 1, we recognized sequences of lithology discontinuities according to the depth variations in the amount and size of coarse fragments (Table 1 and Fig. 3). Pedogenic processes have created a relatively thick (35 cm) argillic-calcic horizon (Btk) with a modest increase in clay relative to the A horizon. An accumulation of secondary carbonates has occurred both as laminations on the bottom of coarse fragments, and as soft masses in the fine earth fraction. In the BC horizons, the

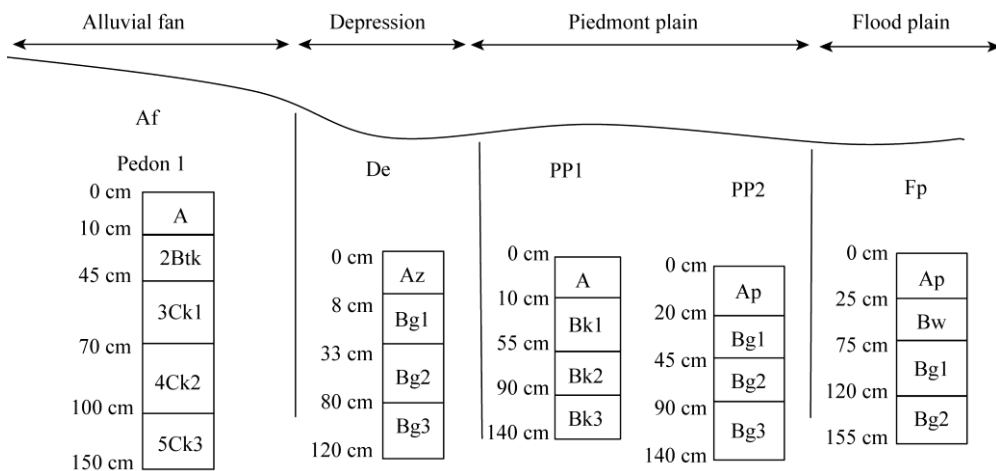


**Fig. 2** Schematic representation of soil pedons locations and their horizons in geomorphic surfaces

**Table 1** Selected physical, chemical and morphological properties of the studied pedons

Horizon	Depth (cm)	Dry color	Clay (%)	Silt (%)	Sand (%)	Gravel (%)	CCE (%)	SOC (%)	EC (dS/m)	Fe <sub>d</sub> (g/kg)	Redness index	Soil texture	pH
Pedon 1, alluvial fan (Af), Typic Calciargids													
A	0-10	7.5YR 5/4	15.0	8.0	77.0	54	14.0	0.3	1.8	3.8	6.0	LS	7.3
2Btk	10-45	7.5YR 5/4	19.0	5.5	75.5	45	15.0	0.6	2.0	4.0	6.0	LS	7.3
3Ck1	45-70	10YR 6/3	12.4	22.9	64.7	66	13.2	0.4	3.8	4.4	0.0	SL	7.9
4Ck2	0-100	10YR 6/3	15.7	42.0	42.3	73	13.2	0.5	3.3	5.0	0.0	L	7.7
5Ck3	100-150	10YR 6/3	15.0	45.0	40.0	62	13.0	0.3	3.2	4.6	0.0	L	7.8
Pedon 2, depression (De), Typic Epiaquepts													
Azg	0-8	7.5YR 5/2	15.7	25.3	59.0	-	13.2	1.7	40.0	7.1	3.0	LS	8.5
2Bg1	8-33	7.5YR 7/2	32.4	51.9	15.7	-	16.4	1.2	2.8	10.2	2.1	SiCL	8.1
2Bg2	33-80	7.5YR 7/2	12.0	72.0	16.0	-	15.1	1.1	2.0	9.5	2.1	SiL	8.1
2Bg3	80-120	7.5YR 7/2	12.5	72.0	14.5	-	13.5	1.0	1.5	10.5	2.1	SiL	8.0
Pedon 3, saline piedmont plain (PP1), Typic Haplocambids													
A	0-10	5YR 5/3	15.6	68.8	15.7	-	15.6	1.7	49.0	5.0	3.0	SiL	8.6
Bk1	10-55	5YR 5/3	12.3	65.4	22.3	-	13.0	1.2	15.8	4.0	3.0	SiL	8.3
Bk2	55-90	5YR 5/3	12.3	72.0	15.7	-	15.1	1.5	10.0	4.0	3.0	SiL	8.1
Bk3	90-145	5YR 5/3	14.0	71.5	14.5	-	14.1	1.1	8.3	4.0	3.0	SiL	8.0
Pedon 4, non-saline piedmont plain (PP2), Typic Endoaquepts													
Ap	0-20	7.5YR 6/3	52.3	32.0	15.7	-	16.6	1.8	1.4	6.0	2.5	C	7.7
Bg1	20-45	10YR 6/1	52.3	35.3	12.3	-	16.6	0.8	1.1	2.3	0.0	C	7.7
Bg2	45-90	2.5YR 6/2	45.7	32.0	22.3	-	16.6	0.4	1.2	5.8	0.8	C	8.1
Bg3	90-140	7.5YR 7/2	35.7	45.3	19.0	-	16.5	0.6	1.0	7.5	2.1	SiCL	8.2
Pedon 5, flood plain (Fp), Typic Aquicambids													
Ap	0-25	7.5YR 6/3	16.0	44.0	40.0	-	13.0	1.0	1.2	3.5	2.5	L	7.9
Bw	25-75	2.5YR 6/4	19.0	42.0	39.0	-	15.6	0.8	1.3	5.3	1.6	L	8.1
Bg1	75-120	2.5YR 6/2	20.0	39.0	41.0	-	12.0	0.5	1.0	5.6	1.6	L	7.1
Bg2	120-155	2.5YR 6/2	17.5	37.0	38.0	5	13.5	0.4	1.0	5.5	2.0	L	8.0

Note: CCE, calcium carbonate equivalent; EC, electrical conductivity; Fe<sub>d</sub>, dithionite-extractable iron; LS, loamy sand; SL, sandy loam; L, loam; SiCL, silty clay loam; SiL, silt loam; C, clay; - means no data.

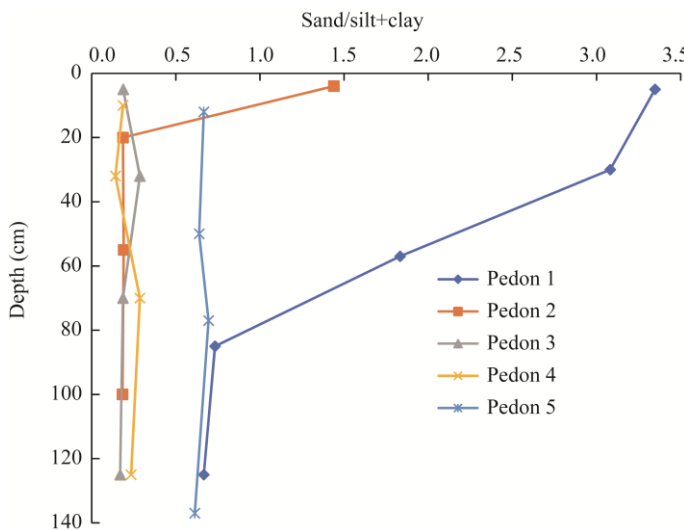


Fig. 3 Vertical variation of sand/silt+clay ratio in the studied pedons

secondary carbonates accumulated under the clasts as carbonates pendants. The secondary carbonates correspond to stage II of the morphogenetic model of Machette (1985) in the lower parts of pedon 1. Carbonate content in pedon 1 varies in a narrow range between 13.0% and 15.0% (Table 1), with the highest in the Btk horizon, which also corresponds to the highest clay content in the pedon. The development of the argillic horizon is generally a time and climate-dependent process (Birkeland, 1999; Ebeling et al., 2016; Bayat et al., 2017b). Hence, the argillic horizon of the pedon 1 is an indicator of long-time landform stability and pedogenesis. The maximum values of RR for the soils are in the surface layers of pedon 1 (Table 1). As values of RR are strongly correlated with the hematite content of soils, these values suggest hematite formation under aerobic conditions and high soil temperature (Schwertmann, 1993; Torrent and Barrón, 1993).

Pedon 2 has been affected by runoff and episaturation (saturation of the soil by water from the surface) from the upslope of the alluvial fans. This pedon has an Az horizon with puffy features, a white veneer of salts on the surface, and very high EC values (40 dS/m). The Az horizon, due to its thickness, does not qualify as a diagnostic salic horizon. The episaturation process also has led to the development of gleyic features in this pedon. In the Az horizon, the sand content is 59%, which decreases to 16% in underlying horizons.

Pedon 3, a loess-derived soil, has been affected by the soluble salts due to its proximity to the depression. EC values in the Az horizon are 49 dS/m, which decreases in the subsurface layers to 8 dS/m. This Az horizon, similar to that in pedon 2, is not a diagnostic salic horizon owing to the low thickness. The secondary carbonates are in the form of thin filaments. Despite the presence of visible secondary carbonates and designation of the subsurface horizons as Bk, they are less than 5% (by volume), and do not meet the criteria of a diagnostic calcic horizon.

The characteristics of pedon 4 in PP2 are distinctly different from the other loessial pedons. Firstly, fluctuations of the ground water table induced the gleyic properties (chroma<2 and mottling). Secondly, EC is considerably lower in this pedon than in pedons 2 and 3, because this pedon has not been affected by the saline water from the upper surfaces. The water table may be charged by both the Hariroud River and the seasonal Karabar River. The difference can be attributed to high clay and low silt content, as well as the transformation of silt to clay.

Pedon 5 is located in the flood plain of the Hariroud River. Based on the particle size distribution, the mixing of the alluvial materials and the loess has occurred. The gleyic and redoximorphic features have developed in the subsurface horizons of the pedon. The most important pedogenic processes in this pedon are the development of structure formation and gleization.

### 3.3 Free iron oxides in the soils

Free iron oxides or dithionite-extractable iron ( $Fe_d$ ) is an indicator of crystalline and amorphous iron oxides (hydroxides) as well as iron bounds to organic materials (Bech et al., 1997; Ortiz et al., 2002; Schaetzl and Thompson, 2015). The  $Fe_d$  content is affected by the nature of parent materials and the types of pedogenic processes. Iron oxides are generally released during the pedogenesis and accumulate in the fine particles (McFadden and Hendricks, 1985; Ortiz et al., 2002).

In pedon 1,  $Fe_d$  content varies between 3.8 and 5.0 g/kg, while in the other pedons, the value is higher, especially in gleyic horizons, and reaches up to 10.5 g/kg in the 2Bg1 horizon of pedon 2 (Table 1). The  $Fe_d$  values in the pedon 1 have been produced during aerated pedogenic conditions, its values are similar to weakly developed pedon 3, and are lower than those of most gleyic horizons in other pedons. During the gleization process, the reduction has led to the release of Fe from Fe-bearing minerals and accumulation as amorphous iron (McFadden and Hendricks, 1985; Schaetzl and Thompson, 2015).

Generally, there is a relationship between  $Fe_d$  and clay content in soils developed on homogenous parent materials (Najafi et al., 2019). The soils in the area developed on three different parent materials of alluvial (pedon 1), loess (pedons 2–4), and a mixture of alluvial and loess (pedon 5). On the other hand, the dominant process in pedon 1 is weathering under aerobic conditions, and on the other pedons the process is gleization. Therefore, there was no correlation between  $Fe_d$  content and particle sizes. As Fe commonly releases from the silt and clay, the relationship between  $Fe_d$  and silt+clay content (Fig. 4) indicates the grouping of the loessial soils together (pedons 2–4), whereas pedons 1 and 5 are classified into separate groups. This result indicates both the effects of parent materials and pedogenic processes on the  $Fe_d$  content.

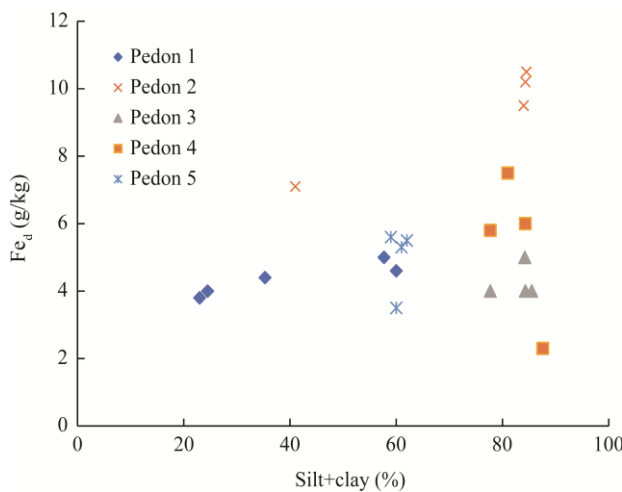


**Fig. 4** Relationship between  $Fe_d$  and silt+clay in the studied pedons

A correlation between  $Fe_d$  content and the redness of soils is mentioned in some researches (McFadden and Hendricks, 1985; Ortiz et al., 2002). However, we did not find any relationships between  $Fe_d$  content and RR values for the soils of the Herat Plain, likely due to the differences in parent materials and hydric pedogenic processes. The lack of correlation between  $Fe_d$  and RR values was also observed in soils of Southwest Barcelona, Spain (Bech et al., 1997).

### 3.4 Micromorphology and clay mineralogy of the soils

The clay coatings on carbonate nodules and coarse particles in the Btk horizon of pedon 1 (Fig. 5a and b) indicate crystallization of nodules prior to clay translocation. The carbonate leaching and clay translocation in calcareous materials require sub-humid climatic conditions with annual precipitation of roughly 400–600 mm (Fedoroff, 1997). Therefore, the occurrence of these processes is the indicator of climatic changes in the region and the polygenetic nature of the soil.

chinaxiv:202211.00144v1

Moreover, in this horizon, the accumulation of iron nodules was observed (Fig. 5c). In the pedon 3, gypsum exists in the form of lenticular euhedral crystals (Fig. 5d).

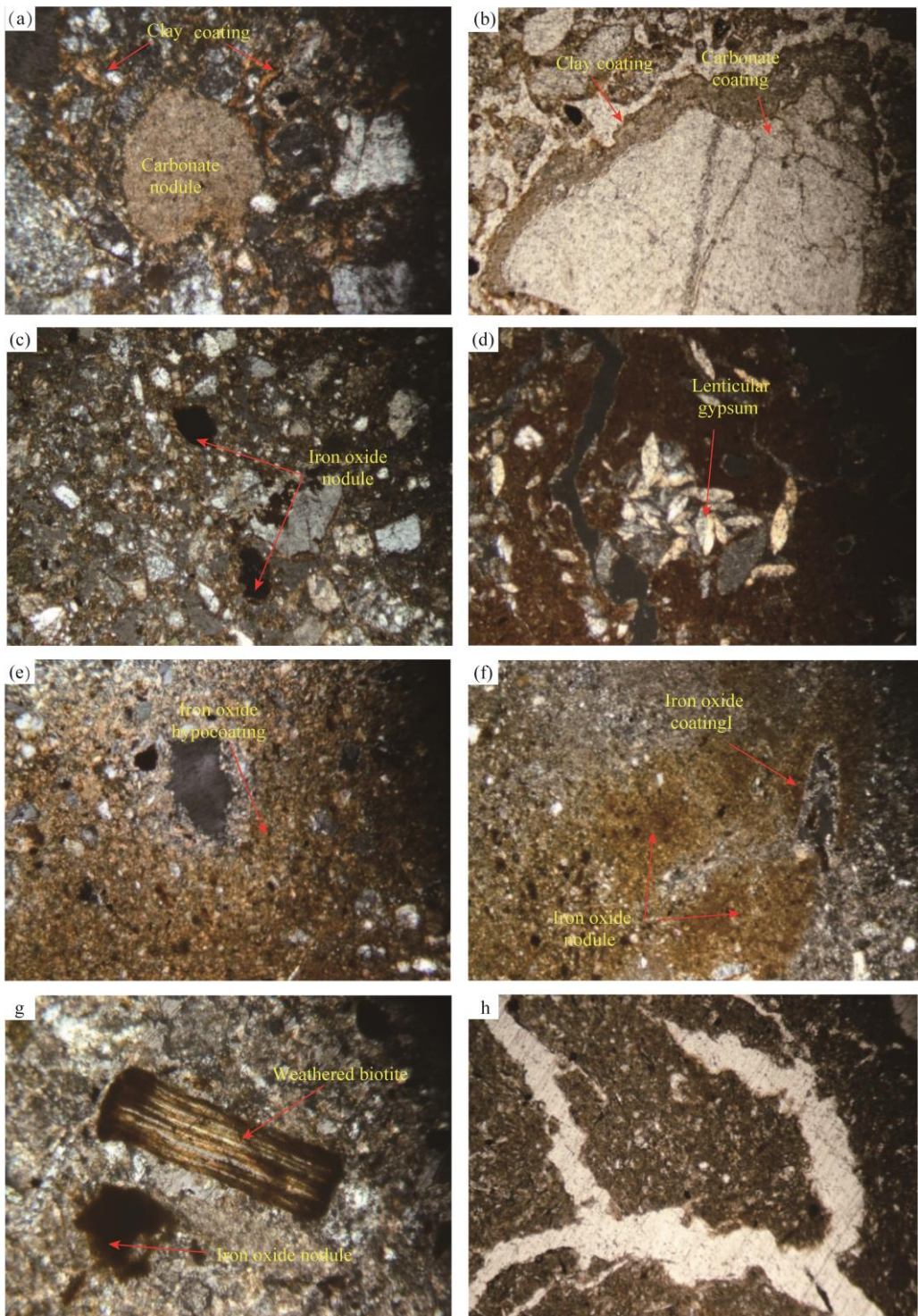


**Fig. 5** (a), clay coating on carbonate nodule (XPL); (b), sequence of clay and carbonate coating on coarse fragment (PPL); (c), iron oxides nodule in the Btk horizon of pedon 1 (XPL); (d), incomplete infilling of lenticular gypsum in the Bk1 horizon of pedon 3 (XPL); (e) and (f), hypocoating and coating of iron oxides (XPL); (g), weathered biotite in the Bg1 horizon of pedon 5 (XPL); (h), subangular blocky microstructure in the Bg1 horizon of pedon 4 (XPL); XPL, crossed-polarized light; PPL, plain-polarized light.

Thin sections of soils in reduced horizons of pedons 4 and 5 show the abundance of iron nodules as well as hypocoatings and quasicoatings of iron oxides (Fig. 5e, f and g). These features indicate reduction status that has led to the deposition of iron nodules, and coatings that is related to weathering and releasing iron from the minerals such as biotite during soil formation (Fig. 5g).

The diffractogram of the Btk horizon of pedon 1 (Fig. 6a) indicates the occurrence of smectite, chlorite, mica-chlorite, kaolinite, and palygorskite mineral in the clay fraction. According to the position and the climatic conditions of the region, it is likely that palygorskite, and to some extent, smectite are the products of pedogenic processes. Neoformation of palygorskite in a Btk horizon in an alluvial fan of central Iran took place under arid/semi-arid and seasonal climatic conditions (Bayat et al., 2017b).

The clay mineralogy of pedon 4 and pedon 5 (Figs. 6d and e) shows higher smectite than those of other pedons, which can be related to the weathering of silt fraction, and increasing both clay content and smectite in clay fraction.

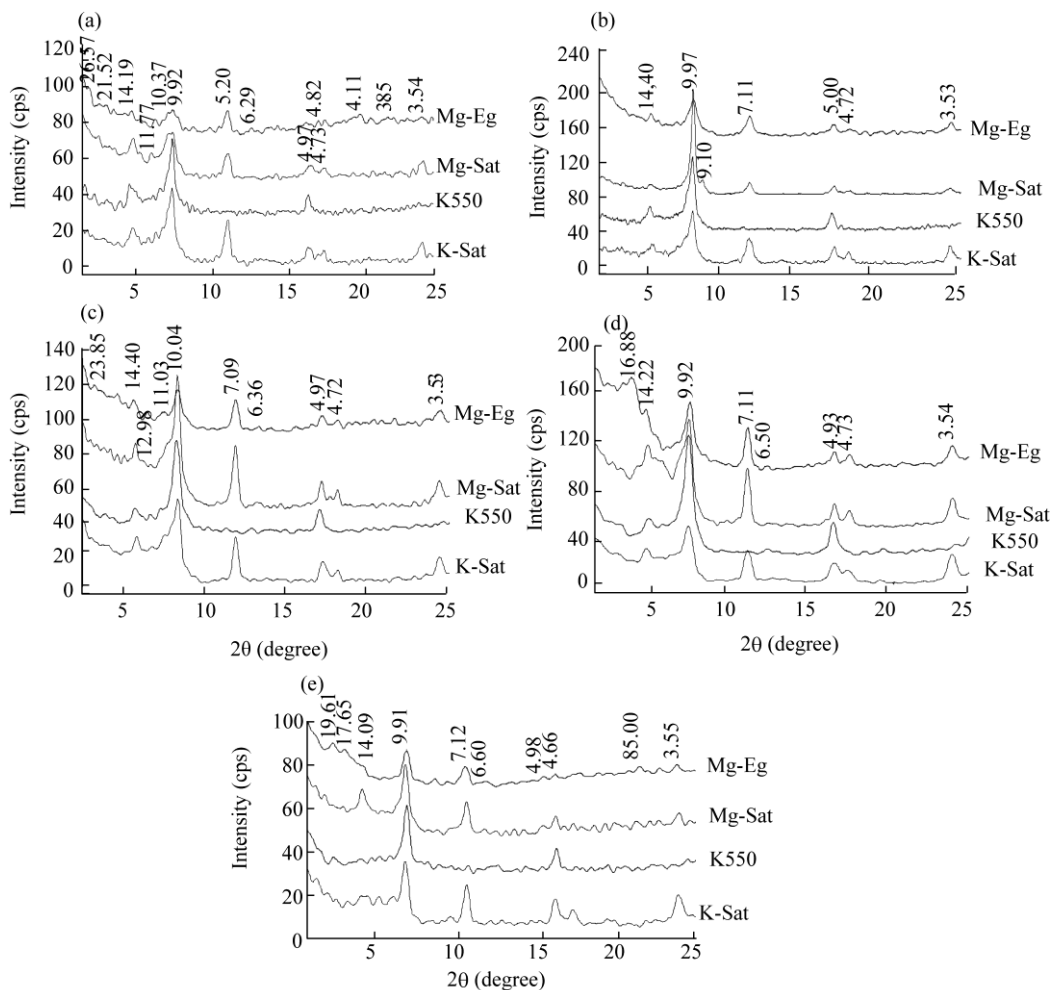


**Fig. 6** (a), X-ray diffraction diffractograms of clay fraction of the Btk horizon of pedon 1; (b), the Bw horizon of pedon 2; (c), the Bk horizon of pedon 3; (d), the Bg1 horizon of pedon 4; (e), the Bg1 horizon of pedon 5; Mg-Sat, Mg satuated; Mg-Eg, Mg and ethylene glycol saturated; K-Sat, K saturated; K550, K saturated and heateh at 550°C; cps, counts per second.

In summary, the clay mineralogy of the soils suggests that palygorskite, and to some extent, smectite are the product of pedogenesis processes, and most of the minerals are inherited from their parent materials. Palygorskite is a magnesium-rich aluminosilicate that is very common in

the soils of arid regions, where MAP is less than 300 mm (Singer, 1980; Neaman and Singer, 2011), because it is stable only under high concentrations of Mg and Si ions with high evaporative and alkaline conditions (Singer, 1980; Kadir and Eren, 2008). Since palygorskite is only stable under climatic conditions with MAP less than 300 mm (Neaman and Singer, 2011). Hence, the occurrence of the mineral is a consequence of the onset of aridity in the region after the development of calcitic nodules and clay coatings in the alluvial soils.

## 4 Discussion

### 4.1 Soil and landscape evolution of the Herat Plain

The sedimentation process of alluvial fan, loess deposition, and fluvial activities of the Hariroud River are the main geomorphological processes in the Herat Plain, which have affected the landscape and soil evolution in the area.

In the Herat Plain, alluvial sediments cover the slopes of the Sepidkuh Mountain in the form of several alluvial fans (Figs. 1a and 2). As tectonic movements are the primary control of fan aggradation (Blair and McPherson, 2009; Bowman, 2019), these sediments are produced during different phases of landscape instability in the region that are probably induced by tectonic movements (Blair and McPherson, 2009) and climatic oscillations. No data is available for the timing of fan deposition and abandonment in western Afghanistan. However, studies in eastern Iran revealed that there was a period of intense fan aggradation between 60 and 40 ka in the region (Walker and Fattahi, 2011; Rashidi et al., 2021). On the other hand, loess deposits have filled the plains of the region (Bohanon and Lindsay, 2007). There are extensive loess deposits in Afghanistan, and their thickness may be up to 50 m (Bal and Buursink, 1976). The Karakum Desert of Turkmenistan and the alluvial plains of the Amu Darya River are mentioned as the source of dust for loess deposits in Afghanistan (Shroder et al., 2011). Loess deposition in Afghanistan generally occurred during the late Pleistocene (Bohannon and Lindsay, 2007) and especially during the last glacial maximum (LGM) (Salem and Hole, 1969). Luminescence dating analyses showed loess sediments in northeastern Iran and near the study area also deposited during LGM until 12 ka (Karimi et al., 2011), and then secondary carbonates formed under cool and moist conditions of early/mid-Holocene (Bayat et al., 2017a). As the morphology of the loess-derived soils in the Herat Plain is similar to loessic soils in northeastern Iran (Karimi et al., 2011), these soils are probably have developed in a similar trajectory.

Calcification, lessivage, and gleization are the main pedogenic processes for the studied soils, which resulted in different soils in the landforms. The most developed soil in the study area was formed in the middle part of the alluvial fan (pedon 1), and the Btk horizon in this pedon is a remnant of past humid climate. In general, the existence of the Btk horizons in calcareous materials of arid regions contains at least three pedogenic sequences including decarbonation, clay production and translocation, and recarbonation (Gvirtzman and Wieder, 2001; Bayat et al., 2017a, 2018). Unlike the Btk horizons in Mediterranean soils of Spain (Ortiz et al., 2002), and alluvial soils of central Iran (Bayat et al., 2017a, 2018), which exhibits the impacts of recarbonation. The Btk horizon in the soils of the Herat Plain formed without recarbonation, and clay coatings formed on carbonate nodules as illustrated by micromorphology analysis (Fig. 1a and b). Clay coatings proceed under long-term warm and sub-humid/humid climate with strong seasonal rainfall that allows clay suspension formation and downward movement of particles by percolating water during moist season and dryness of soil matrix and the precipitation of particles during dry season (Fedroff, 1997; Scarciglia et al., 2006; Ebeling et al., 2016). These processes have mainly occurred during warm and moist interglacial stage in the middle latitudes of Mediterranean (Fedroff, 1997; Scarciglia et al., 2006). On the other hand, calcification process in calcareous soils of mid-latitudes requires MAP between 350 and 450 mm under a semi-arid and seasonal climate (Gvirtzman and Wieder, 2001). Therefore, these processes together with the illuviation of pedogenic iron in alluvial soils suggest that the soils experienced at least two periods with more available moisture during the late Quaternary. The precipitation of clay

coatings on carbonate nodules reveals a shift from semi-arid climate (during carbonation) to sub-humid (during clay illuviation) in the Heart Plain. More studies in the area are required about the timing and magnitude of these episodes.

Loess deposits in the Herat Plain can be considered as a part of a loess belt extending from northeastern Iran (Karimi et al., 2011) to southern Tajikistan (Li et al., 2019). These deposits and their associated soils are formed in response to changes in the patterns and strengths of atmospheric circulations during the late Quaternary (Bayat et al., 2017b; Li et al., 2019). Although loess deposits in the Herat Plain are strongly affected by gleization and redoximorphic processes, calcic horizons in piedmont-plain soils contain signals of paleoclimatic changes in the area. Loess deposition is generally favored by a reduction in the velocity of dust-bearing winds mostly under windy and arid conditions (Karimi et al., 2011; Rhoton and Makewich, 2017). Pedogenic processes modify loess deposits in several ways. Modification of loess deposits and the formation of calcic horizons in the piedmont plain of the study area is strong evidence for post-depositional processes under a moister environment than today. Stable isotopic signals in pedogenic carbonates of northeastern Iran revealed that secondary carbonates in loess deposits of the region precipitated in a mixed ecosystem of C<sub>3</sub>–C<sub>4</sub> plants and a cooler environment (Bayat et al., 2017a).

Authigenic clay minerals also can provide insights into paleoclimatic conditions (Galán and Pozo, 2011; Bayat et al., 2017b). Palygorskite, a fibrous clay mineral, is an Mg-rich aluminosilicate that is very abundant in the soils of arid regions (Churchman and Velde, 2019). There are two main sources for palygorskite in arid soils: inheritance from parent material and autogenesis by neoformation from soil solution or transformation from a precursor mineral (Galán and Pozo, 2011). Because palygorskite occurs in both alluvial and loessic soils of the Herat Plain (Table 2), we imply that the mineral crystallization in the region is independent from the type of parent material and formed by authigenic process. Although saline-alkaline groundwater (especially temporal groundwater) can favor the crystallization of palygorskite (Churchman and Velde, 2019), the mineral was not detected in the gley soils of the Heart Plain. Thus, the mineral formation in the region is controlled by climatic factors. Palygorskite is very sensitive to mean annual precipitation, and is stable only when MAP is less than 300 mm (Neaman and Singer, 2004). Hence, the stability of palygorskite in the soils of the region is evidence of alkaline acidity and high Mg content, which implies the onset of aridity and the trend of increase in environmental aridity in the Heart Plain.

According to geomorphological processes and soil formation, we suggested a conceptual sequence for soil–landscape evolution in the Herat Plain during the late Quaternary: (1) formation of alluvial fan and development of a well-developed paleosol in the climatic setting favorable for weathering and translocation of clay and carbonates leading to the formation of the Btk horizon; (2) accumulation of loess in the Herat Plain and formation of calcic horizon during more humid time, likely occurring in the Holocene; and (3) surface salinization and gleization leading to the development of gleyic properties and formation salic horizons.

## 5 Conclusions

Alluvial and loess-derived soils of the Herat Plain show different morphological and physical-chemical properties in response to diversity in the nature of parent materials, age, and drainage conditions. All the studied soils are calcareous. And calcification, lessivage, and gleization are the most important soil-forming processes in the Herat Plain. Gleization strongly affected the soils of the Herat Plain by episaturation in the depression geomorphic surface and by endosaturation in the non-saline piedmont plain and flood plain geomorphic surfaces. The Btk horizon in the region is characterized by the existence of clay coatings on carbonate nodules, evidence of clay and Fe<sub>d</sub> illuviation as well as the formation of iron nodules. Several lines of evidence for the late Quaternary climatic changes in the Heart Plain have been demonstrated including (1) the development of the Btk horizon in alluvial soils; (2) the deposition of loess

deposits; (3) the formation of calcic horizons in loessic soils; and (4) the formation and preservation of palygorskite in both alluvial and loessic soils. The crystallization and preservation of palygorskite clay minerals in both alluvial- and loess-derived soils imply the onset of aridity and the increasing trend of environmental aridity in the region.

Finally, as the soils of the Heart Plain imply paleoclimatic proxies, we strongly recommend a more detailed study, especially numerical dating of soils and landforms, for Afghanistan, where there is only very limited data on soils, landscapes, and paleoclimate.

## Acknowledgements

This work is supported by the Ferdowsi University of Mashhad, Iran (3/39455: 1394/09/10). We gratefully appreciate Prof. Ronald AMUNDSON for thoughtful reviewing and constructive comments on an earlier version of the manuscript that markedly improved the quality of the paper.

## References

Ahmadi J. 2021. Afghanistan geography: Mountain regions and region-specific soil type, *International Journal of Multidisciplinary Research and Growth Evaluation*, 2(3): 326–328.

Allison L E. 1960. Wet combustion apparatus and procedure for organic and inorganic carbon in soil. *Soil Science Society of America Journal*, 24(3): 36–40.

Bal L, Buursink J. 1976. An inceptisol formed in calcareous loess on the "Dast-i-Esan Top" plain in North Afghanistan. Fabric, mineral and element analysis. *Netherlands Journal of Agricultural Sciences*, 24(1): 17–42.

Bayat O, Karimi A, Khademi H. 2017a. Stable isotope geochemistry of pedogenic carbonates in loess-derived soils of northeastern Iran: paleoenvironmental implications and correlation across Eurasia. *Quaternary International*, 429: 52–61.

Bayat O, Karimzadeh H R, Karimi A, et al. 2017b. Paleoenvironment of geomorphic surfaces of an alluvial fan in the eastern Isfahan, Iran, in the light of micromorphology and clay mineralogy. *Arabian Journal of Geosciences*, 10: 91.

Bayat O, Karimzadeh H R, Eghbal M K, et al. 2018. Calcic soils as indicators of profound Quaternary climate change in eastern Isfahan, Iran. *Geoderma*, 315: 220–230.

Bech J, Rustullet J, Garrigó J, et al. 1997. The iron content of some red Mediterranean soils from northeast Spain and its pedogenic significance. *CATENA*, 28(3–4): 211–229.

Birkeland P W. 1999. *Soils and Geomorphology*. New York: Oxford University Press, 448.

Blair T C, McPherson J G. 2009. Processes and forms of alluvial fans. In: Parsons A J, Abrahams A D. *Geomorphology of Desert Environments*. Dordrecht: Springer, 413–467.

Bohannon R G, Lindsay C R. 2007. Geologic Map of Quadrangle 3462, Herat (409) and Chesht-Sharif (410) Quadrangles, Afghanistan. United States Geological Survey, Open-File Report (409/410) 2005-1104-A.

Bowman D. 2019. *Principles of Alluvial Fan Morphology*. Dordrecht: Springer Nature, 164.

Churchman G J, Velde B. 2019. *Soil Clays: Linking Geology, Biology, Agriculture, and the Environment*. Florida: CRC Press, 276.

Cullen H M. 2005. Climate of southwest Asia. In: Oliver J E. *Encyclopedia of World Climatology*. Dordrecht: Springer, 120–125.

Dixon J B, Schultze D G. 2002. *Soil Mineralogy with Environmental Applications*. Madison: Soil Science Society of America, 866.

Dupree L. 1980. *Afghanistan*. New Jersey: Princeton University Press, 804.

Ebeling A, Oerter E, Valley J W, et al. 2016. Relict soil evidence for profound quaternary aridification of the Atacama Desert, Chile. *Geoderma*, 267: 196–206.

Ellicott K, Gall S. 2003. *Junior Worldmark Encyclopedia of Physical Geography*. USA: Farmington Hills, 832.

Evenstar L, Sparks R S J, Cooper F J, et al. 2018. Quaternary landscape evolution of the Helmand Basin, Afghanistan: Insights from staircase terraces, deltas, and paleoshorelines using high-resolution remote sensing analysis. *Geomorphology*, 311: 37–50.

Fedoroff N. 1997. Clay illuviation in Red Mediterranean soils. *CATENA*, 28: 171–189.

Galán E, Pozo M. 2011. Palygorskite and sepiolite deposits in continental environments. *Description, Genetic Patterns and*

Sedimentary Settings. In: Galán E, Singer E. Developments in Palygorskite-Sepiolite Research. A New Outlook on these Nanomaterials. *Developments in Clay Science*, Vol. 3. Amsterdam: Elsevier, 125–173.

Gee G W, Bauder J W. 1986. Particle size analysis. In: Klute A. *Methods of Soil Analysis, Part 1*. Madison: American Society of Agronomy, 383–411.

Gvirtzman G, Wieder M. 2001. Climate of the last 53,000 years in the eastern Mediterranean, based on soil-sequence stratigraphy in the coastal plain of Israel. *Quaternary Science Reviews*, 20(18): 1827–1849.

Kadir S, Eren M. 2008. The occurrence and genesis of clay minerals associated with Quaternary caliches in the Mersin area, southern Turkey. *Clays and Clay Minerals*, 56: 244–258.

Karimi A, Frechen M, Khademi H, et al. 2011. Chronostratigraphy of loess deposits in Northeast Iran. *Quaternary International*, 234(1–2): 124–132.

Kittrick J A, Hope E W. 1963. A procedure for the particle size separations of soils for X-Ray diffraction. *Soil Science*, 96: 319–325.

Li Y, Song Y, Kaskaoutis D G, et al. 2019. Atmospheric dust dynamics in southern Central Asia: Implications for buildup of Tajikistan loess sediments. *Atmospheric Research*, 229: 74–85.

Machette M N. 1985. Calcic soils of the southwestern United States. In: Weide D I, Faber M L. *Soils and Quaternary Geology of the southwestern United States*. Geological Society of America Special Paper, 203: 1–21.

McFadden L D, Hendricks D M. 1985. Changes in the content and composition of pedogenic iron oxyhydroxides in a chronosequence of soils in southern California. *Quaternary Research*, 23(2): 189–204.

Mehra O P, Jackson M L. 1960. Iron oxide removal from soils and clay by a dithionite-citrate system buffered with sodium bicarbonate. *Clays and Clay Minerals*, 7: 317–327.

Moore D M, Reynolds R C. 1997. *X-Ray Diffraction and the Identification and Analysis of Clay Minerals* (2<sup>nd</sup> ed.). Oxford: Oxford University Press, 400.

Najafi H, Karimi A, Haghnia G H, et al. 2019. Paleopedology and magnetic properties of Sari loess-paleosol sequence in Caspian lowland, northern Iran. *Journal of Mountain Science*, 16: 1559–1570.

Neaman A, Singer A. 2004. The effects of palygorskite on chemical and physico-chemical properties of soils: A review. *Geoderma*, 123(3–4): 297–303.

Neaman A, Singer A. 2011. The effects of palygorskite on chemical and physico-chemical properties of soils. *Developments in Clay Science*, 3: 325–349.

Nelson D W, Sommers L E. 1982. Total carbon, organic carbon, and organic matter. In: Page A L, Miller R H, Keeney D R. *Methods of Soil Analysis. Part 2*. (2<sup>nd</sup> ed.). Agronomy Monograph 9. Madison: ASA and SSSA, 539–577.

Ortiz I, Simon M, Dorronsoro C, et al. 2002. Soil evolution over the Quaternary period in a Mediterranean climate (SE Spain). *CATENA*, 48(3): 131–148.

Rahmani S R. 2014. Creating initial digital soil properties map of Afghanistan. Msc Thesis. Indiana: Purdue University, 65.

Rashidi Z, Karimi A, Murray A, et al. 2021. Late Pleistocene–Holocene pedogenesis and palaeoclimate in western Asia from palaeosols of the Central Iranian Plateau. *Boreas*, 51: 201–218.

Rhoades J. 1996. Salinity: electrical conductivity and total dissolved solids. In: Sparks D L. *Methods of Soil Analysis, Part 3, Chemical Methods*. Madison: ASA and SSSA, 417–435.

Rhoton F E, Markewich H W. 2017. Loess. In: Lal R. *Encyclopedia of Soil Science* (3<sup>rd</sup> ed.). USA: Taylor and Francis, 1356–1369.

Salem Z M, Hole F D. 1969. Soil geography and factors of soil formation in Afghanistan. *Soil Science*, 107(4): 289–295.

Salem Z M, Hole F D. 1973. Some chemical and physical properties of certain soils of Afghanistan. *Soil Science*, 116: 178–190.

Scarciglia F, Pulice I, Robustelli G, et al. 2006. Soil chronosequences on Quaternary marine terraces along the northwestern coast of Calabria (Southern Italy). *Quaternary International*, 156–157: 133–155.

Schaetzl T J, Thompson M L. 2015. *Soils: Genesis and Geomorphology*. Cambridge: Cambridge University Press, 778.

Schoeneberger P J, Wysocki D A, Benham E C. 2012. Field book for describing and sampling soils, Version 3.0. Natural Resources Conservation Service, National Soil Survey Center, Lincoln, NE.

Schwertmann J M. 1993. Relations Between Iron Oxides, Soil Color, and Soil Formation. In: Ciolkosz E J, Bigham U. *Soil Color*. Madison: Soil Science Society of America, 51–69.

Shroder J F, Schettler M J, Weihs B J. 2011. Loess failure in northeast Afghanistan. *Journal of Physics and Chemistry of the*

Earth, 36(16): 1287–1293.

Singer A. 1980. The paleoclimatic interpretation of clay minerals in soils and weathering profiles. *Earth Science Review*, 15(4): 303–326.

Soil Survey Staff. 2014. *Keys to Soil Taxonomy* (14<sup>th</sup> ed.). U.S. Department of Agriculture, Natural Resources Conservation Service, 360.

Stoops G. 2003. *Guidelines for Analysis and Description of Soil and Regolith Thin Sections*. Madison: SSSA, 147.

Stoops G, Marcelino V, Mees F. 2018. Interpretation of micromorphological features of soils and regoliths. Amsterdam: Elsevier Science, 720.

Thomas G W. 1996. Soil pH and soil acidity. In: Page A L. *Methods of Soil Analysis, Part 3. Chemical Methods*. Madison: Soil Science Society of America, 475–490.

Torrent J, Barrón V. 1993. Laboratory measurement of soil color. In: Bigham J M, Ciolkosz E J. *Soil Color. Special Publication No. 31*. Madison: Soil Science Society of America, 21–34.

Wali E, Tasumi M, Sinohara Y. 2021. Classification and digital mapping of soils in a semi-arid region of Afghanistan. *Eurasian Soil Science*, 54: 38–48.

Walker R T, Fattahi M. 2011. A framework of Holocene and Late Pleistocene environmental change in eastern Iran inferred from the dating of periods of alluvial fan abandonment, river terracing, and lake deposition. *Quaternary Science Reviews*, 30(9–10): 1256–1271.